ORGANIC PROCESS RESEARCH & DEVELOPMENT
OPR&D

pubs.acs.org/OPRD

Communication

Continuous Flow *C*-Glycosylation via Metal–Halogen Exchange: Process Understanding and Improvements toward Efficient Manufacturing of Remdesivir

Timo von Keutz, Jason D. Williams,* and C. Oliver Kappe*

Cite This: https://dx.doi.org/10.1021/acs.oprd.0c00370

Read Online

ACCESS | Metrics & More | Article Recommendations | Supporting Information

ABSTRACT: As remdesivir is the first approved treatment for COVID-19 (SARS-CoV-2), its production is likely to be of vital importance in the near future. Continuous flow processing has been demonstrated as a key technology in the manufacturing of high-volume active pharmaceutical ingredients and is considered for use in this synthetic sequence. In particular, the challenging *C*-glycosylation of a pyrrolotriazinamine via metal–halogen exchange was identified as a transformation with significant potential benefit, as exemplified by calorimetric analysis of each reaction step. Multiple simplifications of this process were attempted in batch but in general were found to be unfruitful. The five-feed process was then transferred to a flow setup, where specific conditions were found to circumvent solid formation and permit stable processing. Detailed optimization of stoichiometries provided an improvement upon batch conditions with a total residence time of <1 min.

KEYWORDS: *flow chemistry, organometallics, magnesium–halogen exchange, active pharmaceutical ingredient synthesis, exothermic chemistry*

INTRODUCTION

The rapid spread of the SARS-CoV-2 virus (COVID-19) in the first half of 2020 has caused mass disruption worldwide and an enormous number of cases and deaths, which are unprecedented in recent history.[1] Accordingly, treatments for the disease have been sought mostly as repurposed drugs because they have already passed the initial human safety milestones.[2] Of these potential treatments, remdesivir (**4**), a broad-spectrum antiviral that was originally developed to treat Ebola,[3] has received significant attention, becoming the first treatment to be approved by the U.S. Food and Drug Administration (FDA) and, more recently, receiving approval in Europe.[4] As a result, the demand for this compound will likely be tremendous, requiring an efficient manufacturing route, with the accompanying technology and supply chain in place.[5] Many published studies have already begun to improve or redefine the manufacturing route.[6]

As highlighted in a recent article, synthetic chemistry has a key role to play in managing this pandemic by providing efficient routes to key active pharmaceutical ingredients (APIs).[7] In particular, the global disruption of manufacturing supply chains has encouraged many countries to refocus their efforts to become less reliant on importing key APIs and their intermediates. Implementation of continuous flow technology is anticipated to have significant benefits for API manufacture in the coming years,[8] specifically, increased throughput and added flexibility, which will allow for an agile response in times of dramatically increased demand such as a global pandemic.[9]

The published synthesis of **4** (Scheme 1a) begins with a *C*-glycosylation of iodinated pyrrolotriazinamine **1** performed by transient *N*-TMS protection using an organometallic (traceless) base followed by magnesium–halogen exchange and reaction with 2,3,5-tri-*O*-benzyl-D-ribonolactone (**2**).[3] This step has already been subjected to multiple different synthetic iterations to improve its performance,[10] including lithium–bromide exchange methods, numerous different protecting groups (most notably, some success in initial routes using 1,2-bis(dimethylsilyl)ethane),[11] and a range of additives to improve the selectivity. Despite these efforts, few details have been published, and discussions of the key findings and the finalized route are generally not included. No patent for a manufacturing route exists, but on the basis of evidence in the published literature, the manufacturing route likely includes this *C*-glycosylation transformation.[6a] Alternative synthetic routes have been suggested, such as the use of artificial-intelligence-based synthesis planning software;[12] however, to our knowledge no laboratory data on these routes have been disseminated.

This *C*-glycosylation reaction of **1** with **2** is expected to access substantial benefits by flow processing. The excellent heat- and mass transfer characteristics instilled by continuous processing make this an ideal method of carrying out organometallic chemistry.[13,14] The long addition times required for exothermic reactions in batch can be circumvented, avoiding the need to hold unstable intermediates for prolonged time periods. As a result, these organometallic

Special Issue: Flow Chemistry Enabling Efficient Synthesis

Received: August 15, 2020

Scheme 1. Reported *C*-Glycosylation Process in the Synthesis of Remdesivir[a]

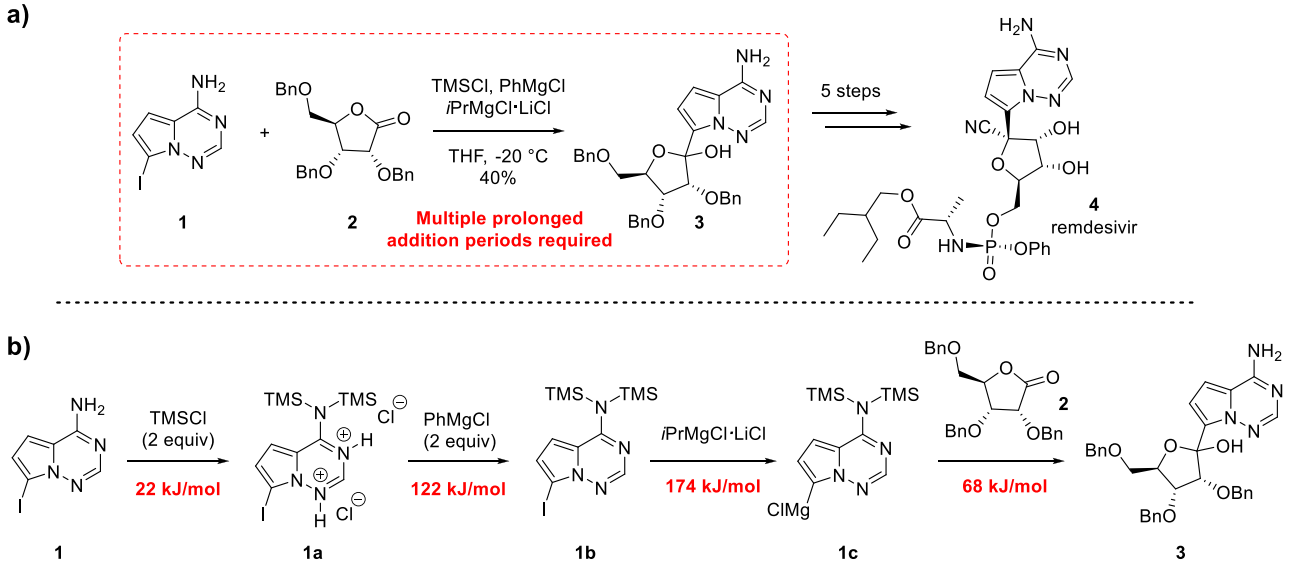

[a](a) The key *C*-glycosylation requires protection of the free NH_2 group in pyrrolotriazinamine **1** followed by metal−halogen exchange and nucleophilic addition to ribonolactone **2** to afford glycosylated pyrrolotriazinamine **3**. A higher yield of 69% has recently been reported for this step performed on larger scale with some process modifications.[6a] (b) A stepwise analysis of the *C*-glycosylation is presented, with the calorimetrically measured exotherm for each reagent addition shown in red, to estimate the total processing time required on a large scale.

reactions can often be performed at a higher temperature in flow compared with batch. Consequently, there can be significant savings in the time and energy consumed in running these processes, alongside the potential for improved impurity profiles. In order to harness these benefits, we endeavored to explore the transformation in detail and undertake the transfer from batch to continuous flow processing.

RESULTS AND DISCUSSION

Initial Process Assessment and Calorimetry Data. Prior to initiation of synthetic efforts, a study was carried out in which the unit operations in this process[3b] were examined. Here the exotherms for the individual reagent additions were measured in separate experiments in order to estimate the required addition periods on the manufacturing scale and gain an appreciation of the potential time savings (Scheme 1b).

First, trimethylsilyl chloride (TMSCl) is added to a solution of iodinated pyrrolotriazinamine **1**. This results in a mild exotherm of 22 kJ/mol. However, more importantly when flow processing is considered, a significant quantity of solid is formed. This solid was found to be the HCl salt of the protected heterocycle (tentative structural representation **1a**; see the Supporting Information for details), resulting from the HCl released from the successive N-silylations.

Next, 2 equiv of a first Grignard reagent is added, resulting in a moderate exotherm of 122 kJ/mol. This reagent is assumed to function as a traceless base to deprotonate the formed HCl salt or, if only 1 equiv of TMSCl is used, to deprotonate the NH. The recorded exotherm period was significantly prolonged, which is proposed to be due to the heterogeneous nature of the suspension of **1a**, meaning that mass transfer limits the rate of this reaction.

To N-protected species **1b** is added a second Grignard reagent, *i*PrMgCl·LiCl, to perform a magnesium−iodide exchange. The resulting aryl Grignard species (proposed structure **1c**, depicted as the MgCl species for simplicity) is the nucleophilic component for *C*-glycosylation. A significant exotherm of 174 kJ/mol was observed, demonstrating the exceptionally fast and energetic nature of this particular exchange reaction.

Finally, the nascent Grignard **1c** is added to a solution of ribonolactone **2**. The resulting exotherm of 68 kJ/mol is moderate in magnitude but occurs quickly. Again, this implies that the manufacturing process will be limited by significantly extended addition periods rather than the actual times required for the individual chemical transformations.

Protection and Magnesium−Halogen Exchange: Attempted Process Modifications. In the analysis of this route, multiple alternative reagents or procedures were identified. Because of the lack of previously published details around this step, it is difficult to discern which of these have been previously attempted and the corresponding results.

First, it was proposed that a bis(*N*-benzyl)-protected starting material would obviate the requirement for in situ TMS protection (Scheme 2a). This would also be cleaved in the later *O*-benzyl deprotection step,[3] meaning that no additional process step would be required. When this *N*,*N*-dibenzylation reaction was carried out, two products were observed: the expected product **5a** was formed alongside the undesired regioisomeric product **5b** (see the Supporting Information for characterization of the two products) in yields of 43% and 49%, respectively.

When the literature glycosylation conditions were employed using the expected regioisomer **5a** (without TMSCl or PhMgCl), a reasonable quantity of the expected adduct was observed (62% by HPLC area). The main side product observed was the protonated (desiodo) species, due to the acidity of ribonolactone **2**. The other regioisomeric starting material **5b** showed a lower yield of the desired product (41% by HPLC area), presumably because of the increased steric hindrance around the nucleophilic center. This approach could

https://dx.doi.org/10.1021/acs.oprd.0c00370
Org. Process Res. Dev. XXXX, XXX, XXX−XXX

Scheme 2. Attempted Modifications of the *C*-Glycosylation Process[a]

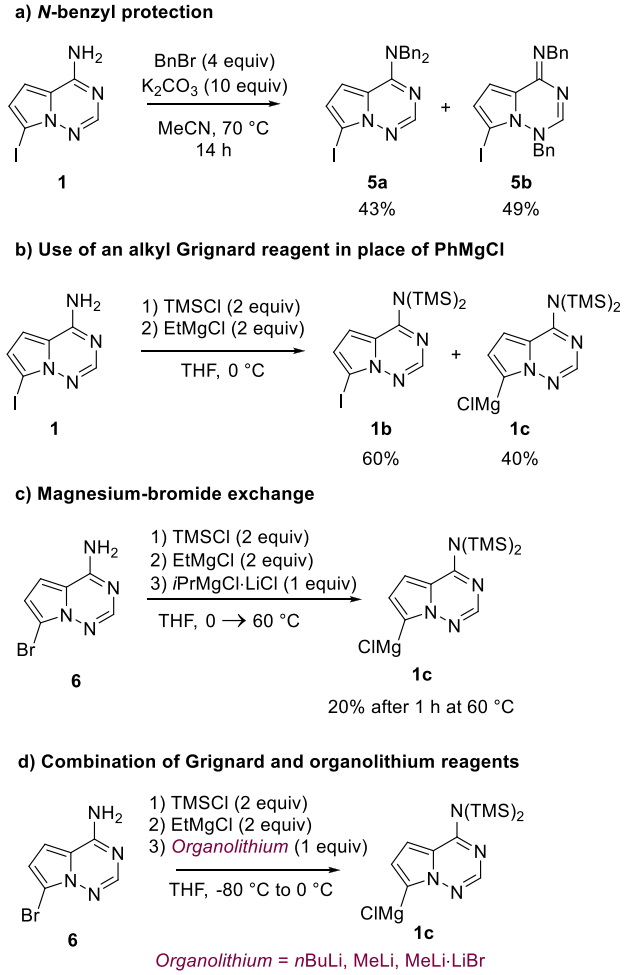

[a](a) *N*-Benzyl protection resulted in two isomers, **5a** and **5b**. Glycosylation of **5a** provided potentially promising results (see the Supporting Information). (b) The use of alkyl Grignard reagents with heteroaryl iodide resulted in a mixture of deprotonation and Mg−I exchange. (c) Unsuccessful Mg−Br exchange provided only minor arylmagnesium formation even at elevated temperatures and lengthened reaction times. (d) Combination of Grignard and organolithium reagents provided irreproducible results or no exchange.

represent a useful method for future work, yet optimization of the *N*-benzyl protection step would be required for it to be synthetically useful.

In the published procedure,[3] PhMgCl is used as a base to facilitate the initial deprotonation/*N*-TMS protection. In view of the relatively high molecular weight of this Grignard reagent and its toxic byproduct (benzene), alternatives were examined. Ideally, it would be possible to simply use 3 equiv of the same Grignard reagent to perform the deprotonation and Mg−I exchange, simplifying the process (Scheme 2b). However, in our hands, the Mg−I exchange appeared to be rapid when an alkyl Grignard (e.g., EtMgCl) was used, even in the presence of two acidic NH groups. The formed heteroaryl Grignard **1c** was observed to quench itself, presumably through deprotonation of an NH in another substrate molecule.

Considering the rapid Mg−I exchange, it was envisaged that this reaction could be performed using heteroaryl bromide **6** in place of the heavier and more expensive iodide **1**. However, the desired Mg−Br exchange was not observed in the presence of *i*PrMgCl·LiCl within 1 h at 0 °C or room temperature. When the reaction mixture was warmed to 60 °C, a small quantity (20% yield) of the desired exchange product was formed in 1 h, rendering this process too slow for use in flow processing even at elevated temperature (Scheme 2c).

Finally, a combination of Grignard reagent (for N protection) and organolithium (for Li−Br exchange) was examined in order to identify a suitable alternative to the current conditions (Scheme 2d). In the case of *n*BuLi, complete exchange was achieved only at −80 °C. Reactions at −40 and 0 °C showed only 46% and 18% Mg−Br exchange, respectively. This was attributed to reaction with the *N*-TMS groups at higher temperatures. Furthermore, these results appeared to be irreproducible and likely were strongly dependent on the addition period, as reported elsewhere.[6b] Alternative organolithium reagents (MeLi and MeLi·LiBr) showed no Li−Br exchange. Since the attempted modifications showed no clear advantage over the originally reported conditions,[3] the original choice of reagents (TMSCl, PhMgCl, and iPrMgCl) were maintained for the transition to flow. It should be noted that because of safety concerns surrounding benzene formation, an alternative Grignard reagent (e.g., tolylmagnesium chloride) would be preferable for larger-scale development work.

Nucleophilic Addition: Impurities and Analysis. After the formation of the heteroaryl Grignard reagent, its addition to 2,3,5-tri-*O*-benzyl-D-ribonolactone **2** furnishes the desired glycosylated compound **3**. As mentioned in previous reports, this step has several key challenges for reaction with an organometallic reagent (Scheme 3). Primarily, the α-proton of this lactone is relatively acidic, favoring deprotonation by the Grignard reagent rather than nucleophilic attack. The products of this pathway are simply the starting pyrrolotriazinamine **7** and the enolate form of lactone **2a**, which returns the starting material **2** upon acidic quench.

Additional complications arising from the proposed ketone intermediate **3a** were also observed. Since this intermediate is more electrophilic than the starting material **2**, it is prone to undergo reaction with the heteroaryl Grignard or any remaining Grignard from the previous step. This results in the two major impurities **8** and **9**, respectively. To control these impurities, it may be advantageous to maintain an excess of lactone **2**.

It is noteworthy that this ketone intermediate **3a** has not been previously proposed but is likely to be present under nonacidic conditions. In the ^{13}C NMR spectrum of product **3** in DMSO-d_6, a signal at 189.0 ppm was observed, clearly indicating the presence of a ketone. In contrast, the NMR spectrum in $CDCl_3$ showed no peaks above 160 ppm, implying the presence of the furanose form **3** (see the Supporting Information for details).

Flow Process Optimization. During the initial reaction analysis, a key focus was placed upon the prevention of solid formation, which would render this process incompatible with straightforward flow processing.[15] Thus, it was identified that the HCl salt (proposed structure **1a**, which arises from mixing the heterocycle **1** with TMSCl) could be avoided by premixing TMSCl with PhMgCl prior to addition of heterocycle **1**. It is assumed that this instantly quenches any formed HCl, so the basic pyrrolotriazinamine nitrogen atoms remain free. The reaction appeared to be unaffected by the time allowed for

https://dx.doi.org/10.1021/acs.oprd.0c00370
Org. Process Res. Dev. XXXX, XXX, XXX−XXX

Scheme 3. Representation of the Reaction Pathway, Including Side Product Formation by Onward Reaction of the Product (Top Arrow) or Simple Deprotonation of Lactone 2 (Bottom Arrow)

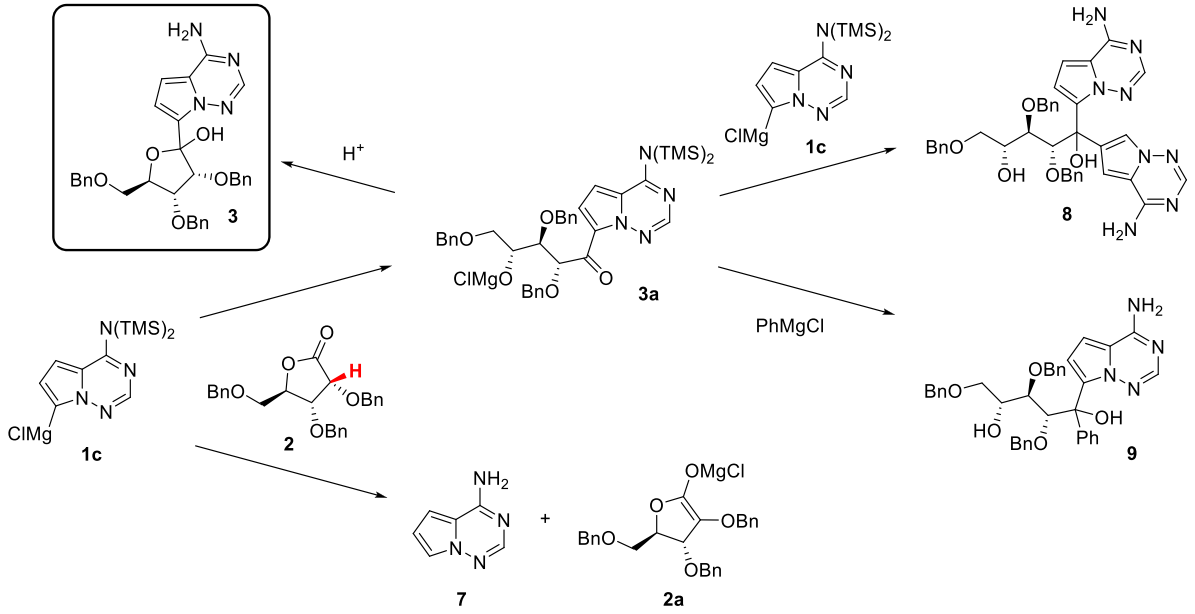

premixing of these reagents, and no solid formation was observed at any point.

By implementing the described change in addition order, it was possible to begin transferring the process to continuous flow. To achieve this, a FlowPlate[16,17] microreactor (Ehrfeld) was used (process plate with "TG" geometry, internal volume 0.4 mL, channel width 0.2 mm in the mixing structure or 0.5 mm in the residence channel; see the Supporting Information for further details) with the aim of providing optimal mass- and heat transfer in a manner that can be maintained for larger-scale processing.[17] The five required reaction streams were mixed as depicted in Scheme 4. The PhMgCl and TMSCl are mixed in a Y-piece prior to entering the FlowPlate reactor because of the low exothermicity and residence time sensitivity of this step. This stream is then mixed with heteroaryl iodide **1**, followed by addition of *i*PrMgCl and then lactone electrophile **2**.

In order to maintain the process intensity, heteroaryl iodide **1** was used as a 0.4 M solution, which is close to its solubility limit in THF (~0.5 M). Similarly, a concentrated solution of TMSCl (2 M) was used, and both Grignard reagents remained undiluted (both 2 M). Initial experiments demonstrated that temperatures below 0 °C could not be used with those concentrations because of the instant formation of solids. During operation at temperatures of 40 °C or above, pressure fluctuation was observed as a result of partial blockages, which resulted in inconsistent reagent delivery and unrepresentative results. Furthermore, it was determined that a significant deficiency of PhMgCl versus TMSCl (1 equiv of PhMgCl and 2 equiv TMSCl) also resulted in solid formation, presumably due to formation of the HCl salt.

With these stoichiometries, experiments were carried out to determine the required residence time for Mg–I exchange. Although the LiCl salt is proposed to provide a higher rate of exchange,[18] *i*PrMgCl itself was found to provide full exchange in a residence time of 2.6 s. This short reaction time enables a high reaction throughput even in a small reactor volume. Furthermore, it appeared as though a short residence time of

Scheme 4. Schematic Layout of "Flow Setup A" Used in This Study[a]

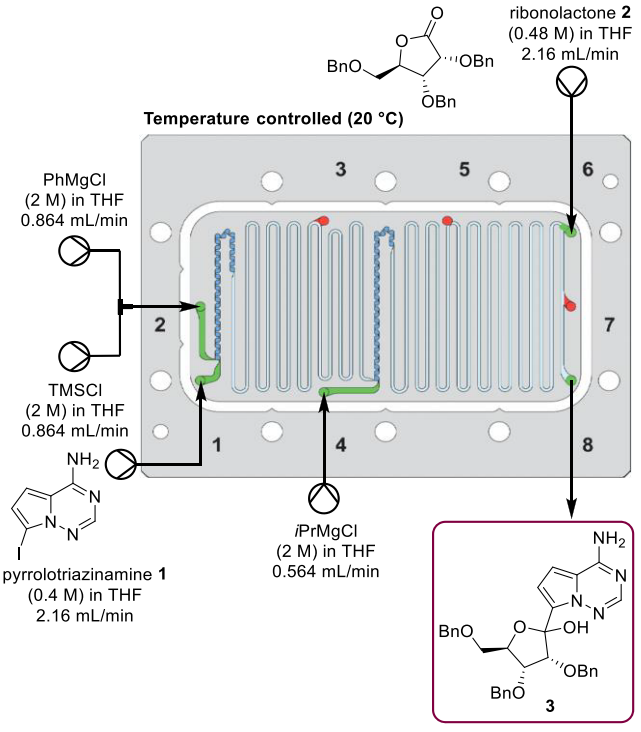

[a]The displayed flow rates correspond to the conditions used in Table 1, entry 2.

~9 s (slightly variable, based on equivalents of reagents used) was sufficient for complete reaction of lactone **2**, since increasing this final residence time unit showed no decrease in quenched heterocycle **7** (see Supporting Information).

The detailed flow optimization began by comparing results versus a benchmark batch reaction carried out as previously described (Table 1, entry 1),[3a] which achieved a 40% yield of

https://dx.doi.org/10.1021/acs.oprd.0c00370
Org. Process Res. Dev. XXXX, XXX, XXX–XXX

Table 1. Summary of Results from Flow Optimization Experiments Using the Conditions Outlined in Scheme 4

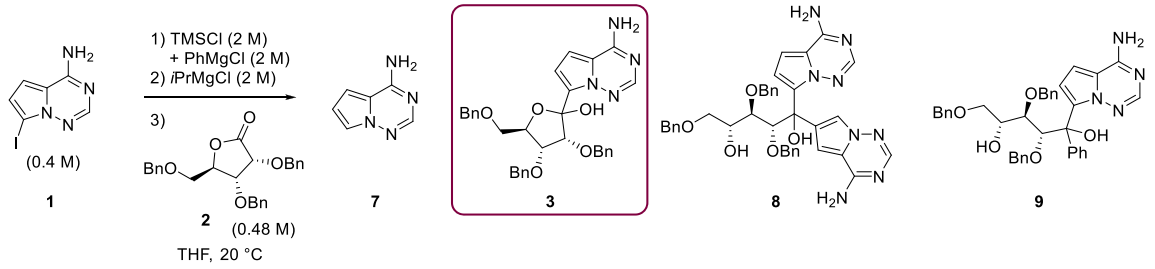

					yields [%][a]				
entry	equiv of TMSCl	equiv of PhMgCl	equiv of *i*PrMgCl	equiv of lactone **2**	**1**	**7**	**desired product 3**	**8**	**9**
1[b]	2	2	1	1	0.1	9.1	**39.6**	15.4	14.0
2[c]	2	2	1.3	–	0.1	**70.3**	–	–	–
3	2	2	1.3	1	0.4	8.2	**12.6**	7.1	43.2
4	2	2	1.3	1.2	0.6	18.4	**21.8**	2.7	23.9
5	2	1.5	1.3	1.2	0.4	25.9	**32.8**	4.7	10.5
6	1.5	1.5	1.3	1.2	0.3	22.9	**30.4**	4.3	14.3
7	1.5	1.2	1.3	1.2	0.6	25.6	**28.7**	3.8	13.9
8[d]	2	1.5	1.3	1.2	0.2	18.7	**33.2**	12.0	7.8
9[e]	2	2	1.3	1.2	3.0	14.1	**39.8**	8.4	13.7
10[e]	2	1.8	1.3	1.2	10.3	12.7	**42.9**	10.2	5.6
11[e]	2	1.5	1.3	1.2	40.1	7.9	**27.9**	12.6	2.2
12[e]	2	1.8	1.4	1.2	3.5	10.1	**46.5**	12.7	7.1

[a]Determined by HPLC area % at 254 nm. [b]The experiment was performed in batch as a benchmark. In this experiment, *i*PrMgCl·LiCl was used. [c]No lactone **2** was added in this experiment to obtain an idea of the performance of the first two reaction steps. [d]A batch quench was used to maintain an excess of **2**. [e]Flow setup B was used, providing additional residence time for the N-protection step.

the desired product **3** by HPLC analysis (corresponding to the reported isolated product yield of 42%), alongside a 9% yield of protonated heterocycle **7**. Side products **8** and **9** were observed in 15% and 14% yield, respectively. It was found that in flow a slightly higher quantity of *i*PrMgCl (1.3 equiv) was required to achieve complete Mg−I exchange.

The first flow experiments were carried out using a 1.6 mL sample loop to inject heterocycle **1**. An experiment was carried without lactone **2** (i.e., simply forming Grignard **1c**, followed by a quench) to determine the performance of these first two steps (entry 2). Although a relatively low purity of the quenched product **7** was observed, the majority of the side products did not absorb at 310 nm, implying that the heterocycle was not incorporated (see the Supporting Information for the corresponding chromatograms). Compared with batch experiments, the first flow experiment including lactone **2** showed a very high quantity of side product **9** (entry 3), although this was found to improve significantly when the number of equivalents of lactone **2** was increased (entry 4).

In an attempt to decrease the quantity of side product **8**, the stoichiometries of PhMgCl and TMSCl were modulated (entries 5−7). Although the quantities of side products **8** and **9** decreased, a significantly higher quantity of the protonated product **7** was observed instead. This signifies problems in the initial N protection. The most favorable of these results was observed when 2 equiv of TMSCl was maintained, but with 1.5 equiv of PhMgCl (entry 5).

It was envisaged that maintaining an excess of lactone **2** throughout the course of reaction may decrease side product **9**. To achieve this, an experiment was attempted in which the Grignard (formed in flow) was added to a batch of lactone **2** (i.e., a "batch quench"). The resulting yield was not a significant improvement on the previous setup (entry 8).

Another consideration was that the N-protection step may be far slower than Mg−I exchange and nucleophilic attack. Accordingly, the TMSCl/PhMgCl stream was combined with heterocycle **1** prior to entering the FlowPlate and was provided an extra 2 mL residence time unit (~38 s; see "flow setup B" in the Supporting Information for details). Gratifyingly, this provided a significant improvement upon the previous results (entry 9). The stoichiometry of PhMgCl was reduced to limit the yield of side product **9** (entries 10 and 11), but some heteroaryl iodide **1** remained since some *i*PrMgCl was now being consumed by the HCl byproduct of N protection. A slight increase in the number of *i*PrMgCl equivalents provided almost complete Mg−I exchange with a lower quantity of **9**. The resulting yield of the desired product **3** was optimal under these conditions (47%; entry 12). These conditions were found to be stable for operation over 17 min (3.8 g, 14.7 mmol of starting material processed) with no pressure fluctuations. Because of the poor commercial availability of pyrrolotriazinamine **7**, a longer scale-out run was, unfortunately, not possible in this setting.

Although the development of this continuous flow procedure has not resulted in a significant yield improvement versus the original published procedure (47% vs 40% HPLC area in our hands),[3a] there is a marked improvement in processability. The batch procedure uses three different temperature regimes (20, 0, and −20 °C) and exotherm-limited addition times, leading to a reaction time of several hours (which would likely be much extended on the manufacturing scale). In contrast, the developed flow procedure uses only a single temperature zone and enables complete reaction in a residence time of <1 min, allowing for

https://dx.doi.org/10.1021/acs.oprd.0c00370
Org. Process Res. Dev. XXXX, XXX, XXX−XXX

high throughput upon scale-up. In order to facilitate this straightforward scale-up, the chemistry was performed in a commercial flow chemistry platform with a defined scale-up strategy.[17]

CONCLUSION

The use of continuous flow processing for organometallic reactions has been proven as an efficient manufacturing technique and may be advantageous for use in the *C*-glycosylation step in the synthesis of remdesivir. The potential advantage was illustrated by a series of calorimetric analyses that demonstrated significant exotherms arising from four sequential reagent addition steps. It was expected that the improved heat transfer afforded by flow processing would allow substantially faster processing of the reaction mixtures.

Upon initial assessment, numerous potential process improvements could be applied in order to streamline this lengthy transformation. Accordingly, a number of these were attempted, and their related drawbacks have been discussed in some detail. Additionally, the main side reactions encountered in this reaction and their associated routes of formation have been analyzed.

Finally, the reaction was adapted to operate under continuous flow conditions. Reaction parameters permitting stable operation were identified, which proved to be a significant challenge because of the numerous possible sites of protonation and potentially insoluble metal salts. It was found that the Mg−I exchange was exceptionally fast in this case, which allowed a residence time of just 2.6 s for this step, with a total residence time of just 56 s for the overall three-step sequence. Further optimization of the reagent stoichiometries suppressed the identified impurities arising from onward reaction of the intermediate, maximizing the quantity of C-glycosylated pyrrolotriazine **3**. This corresponds to a throughput of 51.8 mmol/h for starting material **1**, with a proven scale-up pathway in this reactor using smart-dimensioning concepts.[17] It is envisaged that these results will prove to be valuable to future remdesivir manufacturing efforts toward the goal of effective continuous processing.

ASSOCIATED CONTENT

Supporting Information

The Supporting Information is available free of charge at https://pubs.acs.org/doi/10.1021/acs.oprd.0c00370.

Further details of the reaction setup, experimental results, and characterization data (PDF)

AUTHOR INFORMATION

Corresponding Authors

Jason D. Williams − *Center for Continuous Flow Synthesis and Processing (CC FLOW), Research Center Pharmaceutical Engineering GmbH (RCPE), 8010 Graz, Austria; Institute of Chemistry, University of Graz, 8010 Graz, Austria;* orcid.org/0000-0001-5449-5094; Email: jason.williams@rcpe.at

C. Oliver Kappe − *Center for Continuous Flow Synthesis and Processing (CC FLOW), Research Center Pharmaceutical Engineering GmbH (RCPE), 8010 Graz, Austria; Institute of Chemistry, University of Graz, 8010 Graz, Austria;* orcid.org/0000-0003-2983-6007; Email: oliver.kappe@uni-graz.at

Author

Timo von Keutz − *Center for Continuous Flow Synthesis and Processing (CC FLOW), Research Center Pharmaceutical Engineering GmbH (RCPE), 8010 Graz, Austria; Institute of Chemistry, University of Graz, 8010 Graz, Austria*

Complete contact information is available at: https://pubs.acs.org/10.1021/acs.oprd.0c00370

Funding

The CC FLOW Project (Austrian Research Promotion Agency FFG 862766) is funded through the Austrian COMET Program by the Austrian Federal Ministry of Transport, Innovation and Technology (BMVIT), the Austrian Federal Ministry for Digital and Economic Affairs (BMDW), and the State of Styria (Styrian Funding Agency SFG).

Notes

The authors declare no competing financial interest.

ACKNOWLEDGMENTS

The authors thank René Lebl for additional analytical work.

ABBREVIATIONS

API, active pharmaceutical ingredient; TMS, trimethylsilyl

REFERENCES

(1) (a) Liu, C.; Zhou, Q.; Li, Y.; Garner, L. V.; Watkins, S. P.; Carter, L. J.; Smoot, J.; Gregg, A. C.; Daniels, A. D.; Jervey, S.; Albaiu, D. Research and Development on Therapeutic Agents and Vaccines for COVID-19 and Related Human Coronavirus Diseases. *ACS Cent. Sci.* **2020**, *6*, 315−331. (b) Zhou, P.; Yang, X. L.; Wang, X. G.; Hu, B.; Zhang, L.; Zhang, W.; Si, H. R.; Zhu, Y.; Li, B.; Huang, C. L.; et al. A Pneumonia Outbreak Associated with a New Coronavirus of Probable Bat Origin. *Nature* **2020**, *579*, 270−273.

(2) (a) Maxmen, A. More than 80 Clinical Trials Launch to Test Coronavirus Treatments. *Nature* **2020**, *578*, 347−348. (b) De Savi, C.; Hughes, D. L.; Kvaerno, L. Quest for a COVID-19 Cure by Repurposing Small-Molecule Drugs: Mechanism of Action, Clinical Development, Synthesis at Scale, and Outlook for Supply. *Org. Process Res. Dev.* **2020**, *24*, 940−976.

(3) (a) Warren, T. K.; Jordan, R.; Lo, M. K.; Ray, A. S.; Mackman, R. L.; Soloveva, V.; Siegel, D.; Perron, M.; Bannister, R.; Hui, H. C.; et al. Therapeutic Efficacy of the Small Molecule GS-5734 against Ebola Virus in Rhesus Monkeys. *Nature* **2016**, *531*, 381−385. (b) Siegel, D.; Hui, H. C.; Doerffler, E.; Clarke, M. O.; Chun, K.; Zhang, L.; Neville, S.; Carra, E.; Lew, W.; Ross, B.; et al. Discovery and Synthesis of a Phosphoramidate Prodrug of a Pyrrolo[2,1-*f*][Triazin-4-Amino] Adenine C-Nucleoside (GS-5734) for the Treatment of Ebola and Emerging Viruses. *J. Med. Chem.* **2017**, *60*, 1648−1661.

(4) (a) *First COVID-19 treatment recommended for EU authorisation*, European Medicines Agency, June 25, 2020. https://www.ema.europa.eu/en/news/first-covid-19-treatment-recommended-eu-authorisation (accessed 08-11-2020). (b) *European Commission secures EU access to Remdesivir for treatment of COVID-19*. European Comission, July 29, 2020. https://ec.europa.eu/commission/presscorner/detail/en/ip_20_1416 (accessed 08-11-2020).

(5) (a) On the remdesivir manufacturing process: "The process is both resource- and time-intensive, with some individual manufacturing steps taking weeks to complete." See: *Working to Supply Remdesivir for COVID-19*. Gilead,June 24, 2020. https://www.gilead.com/purpose/advancing-global-health/covid-19/working-to-supply-remdesivir-for-covid-19 (accessed 08-14-2020). (b) Jarvis, L. M. Scaling up remdesivir amid the coronavirus crisis. *Chem. Eng. News*, April 20, 2020. https://cen.acs.org/biological-chemistry/infectious-disease/Scaling-remdesivir-amid-coronavirus-crisis/98/web/2020/04 (accessed 08-14-2020).

(6) During the preparation of this communication, three studies concerning the manufacturing route to remdesivir appeared. See: (a) Vieira, T.; Stevens, A. C.; Chtchemelinine, A.; Gao, D.; Badalov, P.; Heumann, L. Development of a Large-Scale Cyanation Process Using Continuous Flow Chemistry En Route to the Synthesis of Remdesivir. *Org. Process Res. Dev.* **2020**, DOI: 10.1021/acs.oprd.0c00172. (b) Xue, F.; Zhou, X.; Zhou, R.; Zhou, X.; Xiao, D.; Zhong, W.; Gu, E.; Guo, X.; Xiang, J.; Wang, K.; Yang, L.; Qin, Y. Improvement of the C-Glycosylation Step for the Synthesis of Remdesivir. *Org. Process Res. Dev.* **2020**, *24*, 1772. (c) Paymode, D. J.; Cardoso, F. S. P.; Agrawal, T.; Tomlin, J. W.; Cook, D. W.; Burns, J. M.; Stringham, R. W.; Sieber, J. D.; Gupton, B. F.; Snead, D. R. Expanding Access to Remdesivir via an Improved Pyrrolotriazine Synthesis: Supply Centered Synthesis. *Org. Lett.* **2020**, DOI: 10.1021/acs.orglett.0c02848.

(7) Hardy, M. A.; Wright, B. A.; Bachman, J. L.; Boit, T. B.; Haley, H. M. S.; Knapp, R. R.; Lusi, R. F.; Okada, T.; Tona, V.; Garg, N. K.; Sarpong, R. Treating a Global Health Crisis with a Dose of Synthetic Chemistry. *ACS Cent. Sci.* **2020**, *6*, 1017−1030.

(8) For reviews of the advantages of continuous flow processing for API manufacture, see: (a) Gutmann, B.; Cantillo, D.; Kappe, C. O. Continuous-Flow Technology - A Tool for the Safe Manufacturing of Active Pharmaceutical Ingredients. *Angew. Chem., Int. Ed.* **2015**, *54*, 6688−6728. (b) Porta, R.; Benaglia, M.; Puglisi, A. Flow Chemistry: Recent Developments in the Synthesis of Pharmaceutical Products. *Org. Process Res. Dev.* **2016**, *20*, 2−25. (c) Baumann, M.; Baxendale, I. R. The Synthesis of Active Pharmaceutical Ingredients (APIs) Using Continuous Flow Chemistry. *Beilstein J. Org. Chem.* **2015**, *11*, 1194−1219. (d) McWilliams, J. C.; Allian, A. D.; Opalka, S. M.; May, S. A.; Journet, M.; Braden, T. M. The Evolving State of Continuous Processing in Pharmaceutical API Manufacturing: A Survey of Pharmaceutical Companies and Contract Manufacturing Organizations. *Org. Process Res. Dev.* **2018**, *22*, 1143−1166. (e) Berton, M.; de Souza, J. M.; Abdiaj, I.; McQuade, T. D.; Snead, D. R. Scaling continuous API synthesis from milligram to kilogram: extending the enabling benefits of micro to the plant. *J. Flow Chem.* **2020**, *10*, 73−92.

(9) (a) Lee, S. L.; O'Connor, T. F.; Yang, X.; Cruz, C. N.; Chatterjee, S.; Madurawe, R. D.; Moore, C. M. V.; Yu, L. X.; Woodcock, J. Modernizing Pharmaceutical Manufacturing: From Batch to Continuous Production. *J. Pharm. Innov.* **2015**, *10*, 191−199. (b) de Souza, R. O. M. A.; Watts, P. Flow Processing as a Tool for API Production in Developing Economies. *J. Flow Chem.* **2017**, *7*, 146−150. (c) Malet-Sanz, L.; Susanne, F. Continuous Flow Synthesis. a Pharma Perspective. *J. Med. Chem.* **2012**, *55*, 4062−4098.

(10) Numerous patents reporting different variations of this synthetic step have been published, but with relatively little detail. See: (a) Mackman, R. L.; Parrish, J. P.; Ray, A. S.; Theodore, D. A. Methods and Compounds for Treating Paramyxoviridae Virus Infections. US 2011045102, 2011. (b) Butler, T.; Cho, A.; Kim, C. U.; Saunders, O. L.; Zhang, L. 1′-Substituted Carba-Nucleoside Analogs for Antiviral Treatment. US 2009041447, 2009. (c) Mackman, R. L.; Parrish, J. P.; Ray, A.; Theodore, D. A. Methods and Compounds for Treating Paramyxoviridae Virus Infections. WO 2012/012776 A1, 2012. (d) Chun, B. K.; Clarke, M. O. H.; Doerffler, E.; Hui, H. C.; Jordon, R.; Mackman, R. L.; Parrish, J. P.; Ray, A. S.; Siegel, D. Methods for Treating Filoviridae Virus Infections. WO 2016/069826 A1, 2016. (e) Clarke, M. O. H.; Jordan, R.; Mackman, R. L.; Ray, A.; Siegel, D. Methods for Treating Filoviridae Virus Infections. WO 2017/184668 A1, 2017. (f) Chun, B. K.; Clarke, M. O. H.; Doerffler, E.; Hui, H. C.; Jordon, R.; Mackman, R. L.; Parrish, J. P.; Ray, A. S.; Siegel, D. Methods for Treating Filoviridae Virus Infections. US 2019/0275063 A1, 2019. Also see in particular refs 6a and 6b.

(11) (a) Cho, A.; Saunders, O. L.; Butler, T.; Zhang, L.; Xu, J.; Vela, J. E.; Feng, J. Y.; Ray, A. S.; Kim, C. U. Synthesis and Antiviral Activity of a Series of 1′-Substituted 4-Aza-7,9-Dideazaadenosine C-Nucleosides. *Bioorg. Med. Chem. Lett.* **2012**, *22*, 2705−2707. (b) Metobo, S. E.; Xu, J.; Saunders, O. L.; Butler, T.; Aktoudianakis, E.; Cho, A.; Kim, C. U. Practical Synthesis of 1′-Substituted Tubercidin C-Nucleoside Analogs. *Tetrahedron Lett.* **2012**, *53*, 484−486.

(12) For examples of computer-aided synthetic route design toward remdesivir, see: (a) Szymkuć, S.; Gajewska, E. P.; Molga, K.; Wołos, A.; Roszak, R.; Beker, W.; Moskal, M.; Dittwald, P.; Grzybowski, B. A. Computer-Generated "Synthetic Contingency" Plans at Times of Logistics and Supply Problems: Scenarios for Hydroxychloroquine and Remdesivir. *Chem. Sci.* **2020**, *11*, 6736−6744. (b) Lin, Y.; Zhang, Z.; Mahjour, B.; Wang, D.; Zhang, R.; Shim, E.; McGrath, A.; Shen, Y.; Brugger, N.; Turnbull, R.; Jasty, S.; Trice, S.; Cernak, T. Reinforcing the Supply Chain of COVID-19 Therapeutics with Expert-Coded Retrosynthetic Software. *ChemRxiv* **2020**, DOI: 10.26434/chemrxiv.12765410.v1.

(13) For reviews of organometallic chemistry in flow, see: (a) Degennaro, L.; Carlucci, C.; De Angelis, S.; Luisi, R. Flow Technology for Organometallic-Mediated Synthesis. *J. Flow Chem.* **2016**, *6*, 136−166. (b) Colella, M.; Nagaki, A.; Luisi, R. Flow Technology for the Genesis and Use of (Highly) Reactive Organometallic Reagents. *Chem. - Eur. J.* **2020**, *26*, 19−32. (c) Yoshida, J.; Takahashi, Y.; Nagaki, A. Flash Chemistry: Flow Chemistry That Cannot Be Done in Batch. *Chem. Commun.* **2013**, *49*, 9896−9904.

(14) For selected examples of industrially relevant organometallic chemistry in flow, see: (a) Thaisrivongs, D. A.; Naber, J. R.; Rogus, N. J.; Spencer, G. Development of an Organometallic Flow Chemistry Reaction at Pilot-Plant Scale for the Manufacture of Verubecestat. *Org. Process Res. Dev.* **2018**, *22*, 403−408. (b) Hafner, A.; Mancino, V.; Meisenbach, M.; Schenkel, B.; Sedelmeier, J. Dichloromethyllithium: Synthesis and Application in Continuous Flow Mode. *Org. Lett.* **2017**, *19*, 786−789. (c) Hafner, A.; Meisenbach, M.; Sedelmeier, J. Flow Chemistry on Multigram Scale: Continuous Synthesis of Boronic Acids within 1 S. *Org. Lett.* **2016**, *18*, 3630−3633. (d) Hafner, A.; Filipponi, P.; Piccioni, L.; Meisenbach, M.; Schenkel, B.; Venturoni, F.; Sedelmeier, J. A Simple Scale-up Strategy for Organolithium Chemistry in Flow Mode: From Feasibility to Kilogram Quantities. *Org. Process Res. Dev.* **2016**, *20*, 1833−1837. (e) Stueckler, C.; Hermsen, P.; Ritzen, B.; Vasiloiu, M.; Poechlauer, P.; Steinhofer, S.; Pelz, A.; Zinganell, C.; Felfer, U.; Boyer, S.; Goldbach, M.; De Vries, A.; Pabst, T.; Winkler, G.; Lavopa, V.; Hecker, S.; Schuster, C. Development of a Continuous Flow Process for a Matteson Reaction: From Lab Scale to Full-Scale Production of a Pharmaceutical Intermediate. *Org. Process Res. Dev.* **2019**, *23*, 1069−1077.

(15) For a review of oscillatory flow reactors, including their applications in solid handling, see: Bianchi, P.; Williams, J. D.; Kappe, C. O. Oscillatory Flow Reactors for Synthetic Chemistry Applications. *J. Flow Chem.* **2020**, *10*, 475−490.

(16) For selected examples of organometallic chemistry carried out in the FlowPlate reactor, see: (a) Sagmeister, P.; Williams, J. D.; Hone, C. A.; Kappe, C. O. Laboratory of the Future: A Modular Flow Platform with Multiple Integrated PAT Tools for Multistep Reactions. *React. Chem. Eng.* **2019**, *4*, 1571−1578. (b) von Keutz, T.; Cantillo, D.; Kappe, C. O. Continuous Flow Synthesis of Terminal Epoxides from Ketones Using in Situ Generated Bromomethyl Lithium. *Org. Lett.* **2019**, *21*, 10094−10098.

(17) (a) Plouffe, P.; Macchi, A.; Roberge, D. M. From Batch to Continuous Chemical Synthesis-a Toolbox Approach. *Org. Process Res. Dev.* **2014**, *18*, 1286−1294. (b) Mielke, E.; Plouffe, P.; Mongeon, S. S.; Aellig, C.; Filliger, S.; Macchi, A.; Roberge, D. M. Micro-Reactor Mixing Unit Interspacing for Fast Liquid−Liquid Reactions Leading to a Generalized Scale-up Methodology. *Chem. Eng. J.* **2018**, *352*, 682−694.

(18) Krasovskiy, A.; Knochel, P. A LiCl-Mediated Br/Mg Exchange Reaction for the Preparation of Functionalized Aryl- and Heteroarylmagnesium Compounds from Organic Bromides. *Angew. Chem., Int. Ed.* **2004**, *43*, 3333−3336.

https://dx.doi.org/10.1021/acs.oprd.0c00370
Org. Process Res. Dev. XXXX, XXX, XXX−XXX